Oxide muonics: I. Modelling the electrical activity of hydrogen in semiconducting oxides

2006 J. Phys.: Condens. Matter 18 1061

(http://iopscience.iop.org/0953-8984/18/3/021)

INSTITUTE OF PHYSICS PUBLISHING JOURNAL OF PHYSICS: CONDENSED MATTER

J. Phys.: Condens. Matter **18** (2006) 1061–1078 doi:10.1088/0953-8984/18/3/021

Oxide muonics: I. Modelling the electrical activity of hydrogen in semiconducting oxides

S F J Cox[1,2], J S Lord[1], S P Cottrell[1], J M Gil[3], H V Alberto[3], A Keren[1,4], D Prabhakaran[5], R Scheuermann[6] and A Stoykov[6]

[1] ISIS Facility, Rutherford Appleton Laboratory, Chilton, Oxfordshire, OX11 0QX, UK
[2] Condensed Matter and Materials Physics, University College London, WC1E 6BT, UK
[3] Department of Physics, University of Coimbra, P-3004-516 Coimbra, Portugal
[4] Department of Physics, Technion Israel Institute of Technology, 32000 Haifa, Israel
[5] Department of Physics, University of Oxford, OX1 3PU, UK
[6] Paul Scherrer Institute, CH-5232 Villigen PSI, Switzerland

Received 22 July 2005, in final form 7 December 2005
Published 6 January 2006
Online at stacks.iop.org/JPhysCM/18/1061

Abstract

A shallow-to-deep instability of hydrogen defect centres in narrow-gap oxide semiconductors is revealed by a study of the electronic structure and electrical activity of their muonium counterparts, a methodology that we term 'muonics'. In CdO, Ag_2O and Cu_2O, paramagnetic muonium centres show varying degrees of delocalization of the singly occupied orbital, their hyperfine constants spanning 4 orders of magnitude. PbO and RuO_2, on the other hand, show only electronically diamagnetic muon states, mimicking those of interstitial protons. Muonium in CdO shows shallow-donor behaviour, dissociating between 50 and 150 K; the effective ionization energy of 0.1 eV is at some variance with the effective-mass model but illustrates the possibility of hydrogen doping, inducing n-type conductivity as in the wider-gap oxide, ZnO. For Ag_2O, the principal donor level is deeper (0.25 eV) but ionization is nonetheless complete by room temperature. Striking examples of level-crossing and RF resonance spectroscopy reveal a more complex interplay of several metastable states in this case. In Cu_2O, muonium has quasi-atomic character and is stable to 600 K, although the electron orbital is substantially more delocalized than in the trapped-atom states known in certain wide-gap dielectric oxides. Its eventual disappearance towards 900 K, with an effective ionization energy of 1 eV, defines an electrically active level near mid-gap in this material.

1. Introduction: the deep-to-shallow instability of hydrogen and muonium

The theme of this experimental study is the influence of hydrogen impurity on the properties of oxide electronic materials, in the context of the recent realization that interstitial hydrogen may occasionally be a cause of n-type conductivity. This follows the theoretical prediction and

spectroscopic confirmation that hydrogen forms shallow-donor states in the relatively wide-gap oxide ZnO (Van de Walle 2000, Cox *et al* 2001a, Hofmann *et al* 2002, Shimomura *et al* 2002). In a search for further examples of these shallow states, we have begun a systematic survey of other non-magnetic binary oxides, dividing these into two categories. In the present work (Paper I) we report results for the semiconducting oxides, somewhat arbitrarily defined as having a band-gap below the blue-to-ultraviolet boundary at 2.5 eV. Our selection includes Ag_2O, CdO, PbO and RuO_2, for all of which hydrogen-induced electronic conductivity has been explicitly predicted by Kılıç and Zunger (2002). In view of particularly interesting results for Ag_2O, we also include Cu_2O for comparison. In a companion paper (Cox *et al* 2006, referred to below as Paper II) the survey is extended to wide-gap oxides, including several of the high-permittivity materials that might provide an alternative to SiO_2 as nano-scale gate dielectrics.

Hydrogen in semiconductors had formerly been assumed to play the role of a deep-level amphoteric and compensating impurity; that is, to exhibit both donor and acceptor levels deep in the energy gap, trapping charge carriers of either sign to oppose the prevailing conductivity due to shallow dopants. This is the case, for instance, in silicon. It is now apparent that in certain materials, semiconducting and insulating, isolated hydrogen defect centres are close to a deep-to-shallow instability. That is, hydrogen may itself act as a dopant and be a source of n-type conductivity in those materials where it forms shallow donors—as long as it does not also form compensating acceptors. Much of the relevant experimental information comes from studies, not of the hydrogen centres themselves, but of their muonium counterparts, formed following muon implantation in the various materials. This is especially true for the elemental (Group-IV) and binary compound (III–V and II–VI) semiconductors. The positive muon mimics the interstitial proton and, on picking up an electron, forms defect centres analogous to those of neutral monatomic hydrogen. The electronic structures of these paramagnetic states are determined by hyperfine spectroscopy and the corresponding defect levels in the energy gaps estimated from their ionization energies. We make some comments on the methodology in the following section; fuller details of the experimental techniques and the results of previous muonium studies in semiconductors are described in a number of journal reviews: see, for instance, Brewer *et al* (1975), Cox (1987), Patterson (1988), or the more recent summary by Cox (2003).

2. Semiconductor muonics

2.1. The muon–proton and muonium–hydrogen analogies

Use of muonium as an experimentally accessible model for monatomic hydrogen defect centres has several unique advantages. It does not rely on favourable hydrogen solubility, since positive muons (μ^+) can be implanted from a suitable accelerator source into any material. The timescale for data collection is typically 10–20 μs following implantation, set by the muon lifetime of 2.2 μs. This timescale usually favours observation of the isolated defect centres, thus modelling exactly those centres that are primarily responsible for the electrical activity of hydrogen, i.e. the trapping or release of charge carriers. For hydrogen itself, it is typically only a small proportion of the total amount incorporated in a given material that exists as these isolated centres and participates in the interplay of site and charge-state; the majority is paired with other defects or impurities and its primary rôle is passivation, removing electrically active levels from the energy gap. We do not find muonium analogues of passivation complexes in the present work, although examples are known in highly doped III–V semiconductors (Chow *et al* 2001, Lichti *et al* 2003). By comparison with the electronic grade semiconductors that have

been the main focus of muonium studies up to now, however, oxides are notoriously defective materials. The possibility of extrinsic trapping must certainly be borne in mind, notably at vacancies caused not by the muon implantation itself (which, thanks to the lighter muon mass is relatively gentle compared to proton or deuteron implantation, or tritium generation) but by variable stoichiometry.

The nature of muon production and decay is also the basis of the unprecedented sensitivity of μSR spectroscopy, per spin, as compared with that of conventional magnetic resonance. The acronym stands for muon spin rotation, relaxation and resonance, according to the precise variant used (Brewer *et al* 1975). In the present work, we introduce the term *muonics* to describe studies which are specifically designed to model or elucidate the electronic structure and electrical activity of hydrogen impurity, in electronic materials or candidate electronic materials. For this purpose, μSR spectroscopy has the unique advantage of being equally sensitive to neutral (paramagnetic) and ionic (electronically diamagnetic) states of muonium and can follow transitions between these, e.g. by ionization; for hydrogen, this would require some combination of ESR and NMR, solubility permitting.

Although the muon has only one ninth the mass of the proton, muonium properties provide a reliable guide to those of hydrogen as regards local electronic structure, thermal stability and charge-state transitions. The relevant isotope effects are examined critically, for instance, by Cox (2003). The isotope effects would be more severe as regards mobility and diffusion so that (even though monatomic centres are likely to be the important transport states for hydrogen impurity) we make only a passing mention of mobility data in the present account.

2.2. Nomenclature and experimental techniques

We use the accepted chemical symbol Mu for muonium, denoting the neutral state Mu^0 where necessary for emphasis—this may either be the atomic state or any derivative paramagnetic defect centre, deep or shallow. We denote the charged states Mu^+ and Mu^-, by analogy with the interstitial proton and hydride ion, respectively; these are electronically diamagnetic. Explicitly, neutral muonium corresponds to the bound state of the positive muon with a single electron, $Mu^0 = [\mu^+e]$, and the negative ion to that with two (spin paired) electrons, $Mu^- = [\mu^+ee]$. We reserve the notation μ^+ for the purposes of these definitions, or otherwise for the free incoming or energetic particles (and we make no use of negative muons, μ^-, in this work). Just as protons cannot remain free in condensed matter, thermalization as the positive ion also involves a lowering of its energy by association with electrons, which we emphasize by the change from Greek to Roman notation: $\mu^+ \rightarrow Mu^+$. In oxides, unless stabilized at a cation vacancy by a favourable Madelung potential, the muon will undoubtedly mimic protonation of the oxygen anion, forming an analogue of the hydroxide ion (OH^-):

$$\mu^+ + O^{2-} \rightarrow OMu^-. \tag{1}$$

The chemical expectations for hydrogen, the interplay of site and charge state, and the hypothetically important rôle of the hydride ion are all issues of current and contentious debate for dielectric oxides; these and the muonium analogies are discussed at greater length in Paper II.

Neutral muonium can either form promptly on muon implantation, the incoming muon stripping electrons from host atoms while still at epithermal energies, or else following its thermalization as the positive ion, by capture of a radiolytic electron. The question is discussed further by Storchak *et al* (2004) and we find indications of both mechanisms in our data. Central to the present work is the interplay between the various charge states, especially the temperature dependence of the neutral and ionic fractions. Our time-window for data collection at the

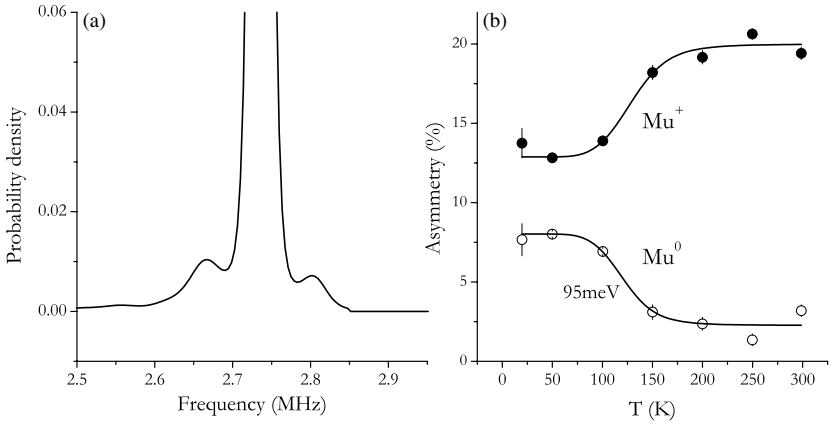

Figure 1. μSR spectrum for CdO at 7 K, obtained as a maximum entropy transform of the 20 mT muon spin rotation signal (a) together with the variations with temperature of the paramagnetic (Mu^0) and diamagnetic (Mu^+) fractions (b), these corresponding to the satellites and central line, respectively.

ISIS pulsed muon source begins only some 100 ns after muon implantation, so that the initial Mu^0, Mu^+ and Mu^- fractions can be determined by thermal processes (i.e. be temperature dependent) if the charge-state transitions are faster than this; otherwise the approach to thermal equilibrium can be monitored explicitly, the data-gate extending typically to 15 μs, 20 μs at most.

A number of the techniques of μSR spectroscopy are well illustrated in the present work, notably muon spin rotation in the case of CdO (section 3), various forms of muon spin relaxation and resonance in Ag_2O (section 4) and muon spin relaxation and repolarization in Cu_2O (section 5). A summary description of preliminary results has been given at conferences held in summer 2004 (Cox *et al* 2005a, 2005b).

3. CdO

CdO is a semiconductor which has a direct gap of 2.4 eV but a much smaller indirect gap in the vicinity of 0.8 eV (Koffyberg 1976, Madelung 1996). Our sample was the purest available powder (99.998%) from Alfa Aesar. At room temperature, the muon spin rotation spectrum exhibits a single narrow line at the muon Larmor frequency. That is, the time-domain signal resembles a cosine wave with little damping: nuclear magnetism is weak in this material, as in all the II–VI compounds, so dipolar broadening of the frequency spectrum is negligible.[7] This spectrum accounts for the full incoming muon polarization, so that all the implanted muons thermalize in an electronically diamagnetic state, presumably via reaction (1). At cryogenic temperatures the spectrum develops hyperfine satellites, shown in figure 1. Such satellites provided the signature for shallow-donor muonium states in ZnO and other members of the II–VI family, namely CdS, CdSe and CdTe (Gil *et al* 2001a). The central line represents muons that still thermalize as OMu^-, constituting positive charge defects in the lattice. The satellites represent those that pick up an electron to form neutral muonium centres (denoted Mu^0 for

[7] Muon spin rotation signals resemble the free-induction decays of proton NMR, more usually with T_2 relaxation clearly visible, though detected via the muon decay rather than by induction in pick-up coils. Our experiments use transverse fields of between 2 and 20 mT, giving Larmor frequencies $(\gamma_\mu/2\pi)B$ in the MHz region (the muon gyromagnetic ratio, $\gamma_\mu = 2\pi \times 0.136$ MHz mT^{-1}, being about three times that of the proton).

emphasis): these are paramagnetic, so that the muon experiences a hyperfine field which adds to or subtracts from the externally applied field, according as to whether the electron is captured spin-up or spin-down.

3.1. Muonium hyperfine and ionization parameters

The satellite splitting or separation that appears as about 140 kHz in figure 1(a) is a polycrystalline average: this frequency spectrum has been obtained for a powder sample of CdO by a maximum-entropy transform (adapted for μSR by Dickson 1999) of the precession signal. It is from analysis of the time-domain signal that we obtain precise values of the hyperfine parameters (using a procedure described by Alberto *et al* 2001): assumption of uniaxial anisotropy gives a contact interaction of $A_{\rm iso} = 48 \pm 4$ kHz and a dipolar component of $D = 106 \pm 7$ kHz. These parameters relate to the principal values of the hyperfine tensor in the usual manner: $A_{\rm iso} = \frac{1}{3}(A_\parallel + 2A_\perp)$ and $D = \frac{2}{3}(A_\parallel - A_\perp)$. The contact interaction seems roughly appropriate to a shallow-donor state—it is some four powers of ten smaller than the hyperfine constant for vacuum-state muonium, $A_0 = 4.5$ GHz. The satellites persist to somewhat higher temperature than in the other four II–VI compounds, disappearing only in the temperature range 100–200 K with a rather large activation energy of 95 ± 18 meV. The evolution of amplitudes, corresponding to the three main spectral lines but again fitted in the time-domain signal, is shown in figure 1(b). The sum of the satellite amplitudes is taken as a measure of the paramagnetic Mu^0 fraction, i.e. of the undissociated donor, and the amplitude of the central line as the diamagnetic Mu^+ fraction, i.e. the ionized donor. Their variations are seen to be complementary: they have been fitted here simultaneously in an equilibrium model (described by Gil *et al* 2001a), assuming no compensation of the muonium donors. The alternative assumption of local compensation would give about half this activation energy. In round figures, therefore, we estimate the donor depth as lying between 50 and 100 meV.

3.2. Comparison with the hydrogenic model for CdO

In the effective-mass approximation, the expectation for the shallow-donor depth or binding energy is

$$R^* \approx R_y(m^*/m_{\rm e})/\varepsilon_{\rm r}^2. \tag{2}$$

Here $R_y = 13.6$ eV is the Rydberg constant or hydrogen ionization potential, which (ignoring a small isotopic correction) is also the electron–muon binding energy in a free muonium atom; m^* is the conduction-electron effective mass, which is somewhat uncertain in CdO, values between 0.11 and 0.33 $m_{\rm e}$ being cited in standard tables (e.g. Madelung 1996). In polar media, the permittivity or dielectric constant $\varepsilon_{\rm r}$ should be given its low-frequency value if R^* is less than the energy $h\nu_{\rm TO}$ of transverse optical phonons (which is commonly the case) but its high-frequency value otherwise (see e.g. Ridley 1982). Using the static value, $\varepsilon_{\rm r}(\omega \to 0) = 21.9$, equation (2) predicts R^* to lie between 3 and 9 meV only—well below our experimental estimate of 50–100 meV. This latter is greater than the 30 meV optical phonon energy, however, (30 meV being equivalent to $\nu_{\rm TO} = 7.8$ THz as cited by Madelung 1996, or $h\nu_{\rm TO} = 262$ cm^{-1} by Stoneham and Dhote 1997) so that use of the optical dielectric constant may be justified in this case. Certainly this gives a consistent picture: setting $\varepsilon_{\rm r}(\omega \to \infty) = 5.3$ in equation (2) predicts R^* to lie between 50 and 150 meV.

Another possibility that should be considered, given the defective nature of CdO, is that the spin density is localized extrinsically some distance away from the muon. CdO is reported to be naturally n-type with a high concentration of cadmium interstitials and oxygen vacancies (Jarzebski 1973, Koffyberg 1976). For hydrogen, a comparable case is the complex with a

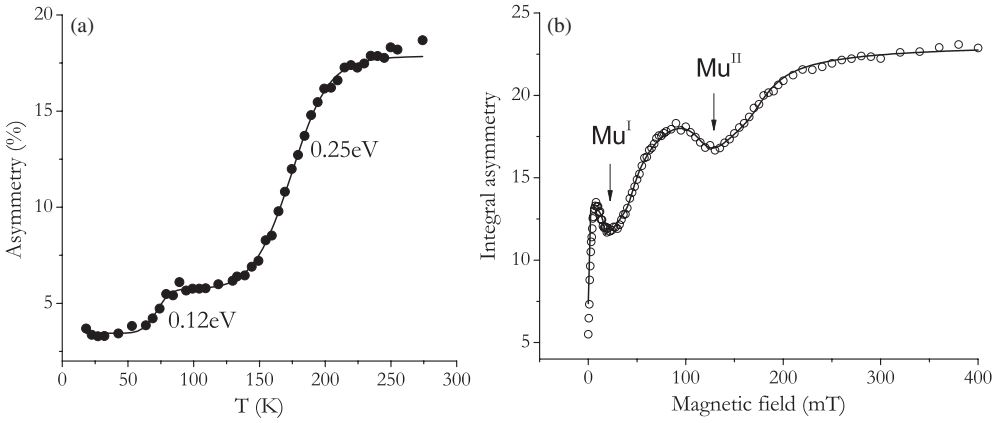

Figure 2. μSR data for Ag_2O, characterizing (a) the diamagnetic and (b) the paramagnetic muonium fractions. These data were recorded at ISIS in transverse (a) and longitudinal (b) magnetic fields, with full polarization corresponding to muon decay asymmetries of about 19% and 23%, respectively. In (a), the variation with temperature is fitted with two thermally activated steps; in (b), the repolarization (here at 120 K) is fitted with a reaction sequence involving three muonium states, two of which exhibit level-crossing resonances in this field range.

vacancy in diamond, giving a low proton hyperfine constant in what is nonetheless a deep centre (Glover *et al* 2004). Vacancy trapping is likewise known for both hydrogen and muonium in silicon (Bech Nielsen *et al* 1997, Schefzik *et al* 2000) but the hyperfine parameters as well as the thermal stability suggest deep centres. Our donor depth of between 50 and 100 meV for CdO certainly appears shallow in this context; it is also quite distinct from the 0.4 eV depth of a narrow impurity band reported by Hogarth (1951) and from the 0.75 eV activation energy for electron generation from point defects above 800 K, reported by Jarzebski (1969).

4. Ag_2O

Silver (I) oxide, Ag_2O, is a semiconductor with a direct bandgap varying between 1.2 eV at ambient temperature and 1.6 eV at cryogenic temperatures—values which are similar to those of important electronic materials such as GaAs, InP and CdTe (see, for example, Madelung 1996). A literature and internet search on silver oxide yields a preponderance of advertisements for battery material, together with descriptions of a surprising variety of other uses, e.g. in medicine and purification, photography, catalysis and the manufacture of electronic materials. It is this latter topic which motivates the present study, coupled with the fact that Ag_2O heads the list compiled by Kılıç and Zunger (2002) of oxides susceptible to hydrogen doping. Whereas the prediction of these authors for CdO is based on first-principles computation of the hydrogen pinning level, for Ag_2O it rests on the assertion of a universal pinning level and its extrapolation onto older electrochemical data. (The latter is true also of the predictions for PbO and RuO_2 considered below.)

4.1. Level crossing and RF resonance

Referring to figure 1(a) for CdO, no such shallow-donor satellites are visible in the muon spin rotation spectrum for Ag_2O at low temperature, but neither is the full muon polarization accounted for. (The sample was also high-purity powder from Alfa Aesar.) Full amplitude of the diamagnetic signal is recovered only towards room temperature, as shown in figure 2(a).

The missing fraction is undoubtedly neutral muonium in some form, and to reveal the nature of this paramagnetic fraction we resort to measurements of muon polarization in longitudinal magnetic fields (i.e. in fields applied parallel to the initial polarization—at ISIS, in-line with the muon beam). Figure 2(b) shows data at 120 K, just below the ionization régime. Time-average measurements of the forward–backward asymmetry in the muon decay, taken as a function of field, reveal two striking dips in polarization known as level crossing resonances.

Two distinct types of resonance must be distinguished, as discussed, for instance, by Kreitzman and Roduner (1995), Roduner (1999). The fields for both types are given approximately by the common formula

$$B_{\mathrm{res}} = \pi \left| \frac{A_\mu + (\Delta \mathrm{M} - 1)A_\mathrm{n}}{\gamma_\mu + (\Delta \mathrm{M} - 1)\gamma_\mathrm{n}} \right|. \tag{3}$$

Here A_μ and A_n are the hyperfine constants in frequency units for the muon and an adjacent nucleus, γ_μ and γ_n their respective gyromagnetic ratios. Setting $\Delta \mathrm{M} = 1$, corresponding to transitions of the muon spin alone, gives the condition known as the pure-muon resonance. At this field, a crossing of the muonium energy levels is avoided—i.e. a degeneracy is lifted—if the muon–electron hyperfine interaction is not perfectly isotropic. One can say that the applied field tunes out parallel components of the hyperfine field here, leaving the muon spin free to precess about transverse components. Setting $\Delta \mathrm{M} = 0$, on the other hand, corresponds to resonant cross relaxation between the muon and adjacent nuclear spins, mediated by their separate hyperfine couplings to the unpaired electron. Whereas a degree of anisotropy of the muon hyperfine interaction is necessary for detection of $\Delta \mathrm{M} = 1$ resonances, $\Delta \mathrm{M} = 0$ resonances are visible for purely isotropic couplings (Kreitzman and Roduner 1995).

It is tempting to assign the two resonances of figure 2(b) to $\Delta \mathrm{M} = 1$ and $\Delta \mathrm{M} = 0$ level crossings of the same muonium state, thereby characterizing spin density both on the muon and on the surrounding Ag nuclei. No satisfactory fitting can be achieved in this single-state model, however, both resonances being too strong and too broad to qualify for $\Delta \mathrm{M} = 0$. Instead, a good fit to the resonances can be achieved if they are both of type $\Delta \mathrm{M} = 1$, that is, if they represent two separate muonium states, which we call Mu^{I} and $\mathrm{Mu}^{\mathrm{II}}$. Their positions at 20 and 130 mT can be seen to correspond to hyperfine constants in the vicinity of 7 and 35 MHz, respectively, equation (3) then simplifying to $|A_\mu| \sim (\gamma_\mu/\pi)B_{\mathrm{res}}$, with $\gamma_\mu = 2\pi \times 136\ \mathrm{kHz\ mT^{-1}}$. The cusp-like and lop-sided appearance to the lineshapes represent the effects of anisotropy in polycrystalline spectra (not unlike the powder-pattern spectra familiar in conventional ESR). Precise hyperfine parameters may be obtained from a detailed fitting of the lineshapes: those corresponding to the fitted curve of figure 2(b) include the effects of transitions between the different states (Lord 2006, Lord *et al* 2006). They are given in table 1 and compared with those of various other muonium defect centres in the concluding section.

Corroborating this assignment, figure 3 shows the prediction and confirmation of radio-frequency (RF) resonances from two separate muonium states. Spectra for Mu^{I} and $\mathrm{Mu}^{\mathrm{II}}$, simulated using hyperfine parameters from figure 2(b), were found to match the RF data closely, both as regards their positions and distinctive lineshapes. The resonance for Mu^{I} dominates in intensity, as though it is the final state in a reaction sequence.

For comparison, longitudinal-field data for muonium in HgO shows a single $\Delta \mathrm{M} = 1$ resonance at 60 mT, visible up to about 170 K (Cox *et al* 2001b). The corresponding contact term is $A_{\mathrm{iso}} = 15$ MHz and the dipolar parameter $D = 5$ MHz. In the case of HgO, however, distinctive frequencies corresponding to this state are visible in the transverse-field muon spin rotation spectrum, recorded at the Swiss Muon Source (Gil *et al* 2001b)—higher frequencies are visible at this continuous muon source than at the ISIS pulsed source. No such additional frequencies could be seen in spectra for $\mathrm{Ag_2O}$, either at ISIS or at PSI,

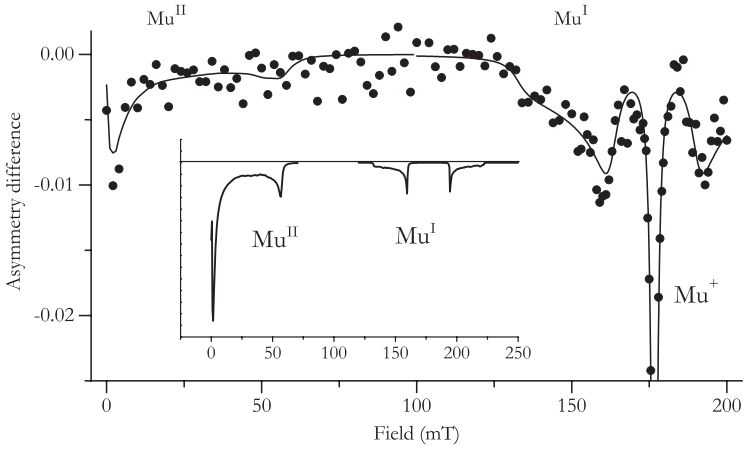

Figure 3. ISIS RF resonance data for Ag_2O, recorded at 120 K. This is the change of forward-backward asymmetry in the muon decay as a 24 MHz RF field is switched on and off. The inset shows simulations using the Mu^I and Mu^{II} hyperfine parameters from figure 2(b). The fitted curve refines the parameters for Mu^I, which appears to be the dominant final state. A resonance of the diamagnetic Mu^+ state is visible at 177 mT.

Table 1. Hyperfine parameters for relevant muonium defect centres, listed in decreasing order of the isotropic component or contact interaction, A_{iso}. Anisotropy is quantified by the dipolar term D. The sign of the contact interaction is so far unknown for muonium in HgO but, by analogy with bond-centred muonium in Si, could well be negative. Spin density ρ_μ on the muon is expressed as the ratio A_{iso}/A_0, where $A_0 = 4463$ MHz is the vacuum-state or free-muonium hyperfine constant. Spin density ρ_n in s, p or d orbitals on the nearest-neighbour nuclei is likewise the ratio of the nuclear hyperfine parameters and the corresponding atomic values, these latter given by Moreton and Preston (1978). Literature references are (i) Patterson (1988), (ii) Schneider *et al* (1990) (the ρ_n s are for Cu neighbours here; these authors also give the values for Cl), (iii) Cox and Symons (1986), (iv) Kiefl *et al* (1988), (v) Gil *et al* (2001b), (vi) Cox *et al* (2001b), (vii) Cox *et al* (2001a), (viii) Alberto *et al* (2001), and (ix) Lord *et al* (2001); a compendium of other literature data for ZnO is given by Cox (2003). Also tabulated are parameters for the silver–hydrogen radical cations: (x, xi) Eachus and Symons (1969), (1970).

	A_{iso} (MHz)	D (MHz)	ρ_μ or ρ_p	ρ_n (s)	ρ_n (p or d)	Reference
Si:Mu_T	2066	0	0.46			(i)
Cu_2O	1280 ± 20		0.29	0.035		
CuCl	1226	0	0.27	0.007	0.14	(ii)
Ag_2O:Mu^{III}	500	300	0.01			
Si:Mu_{BC}	-67	51	-0.015	0.02	0.18	(iii, iv)
Ag_2O:Mu^{II}	37 ± 0.2	10 ± 0.1	0.008			
Ag_2O:Mu^I	7.4 ± 0.1	5	0.002			
HgO	$(\pm)$ 15	5	± 0.003			(v, vi)
ZnO	0.5	0.26	10^{-4}	$\sim 10^{-4}$		(vii, viii, ix)
CdO	0.05	0.1	10^{-5}			
$(\dot{Ag}H)^+$			0.55	0.14	~ 0.3	(x)
$^{\cdot}(Ag–H–Ag)^{2+}$			0.05	0.44		(xi)

even in fields high enough to decouple the ^{107}Ag and ^{109}Ag nuclear moments. Evidently the paramagnetic muonium states in Ag_2O are formed too slowly or are too short-lived for transverse-field spectroscopy, whence the value of the longitudinal-field method. This latter

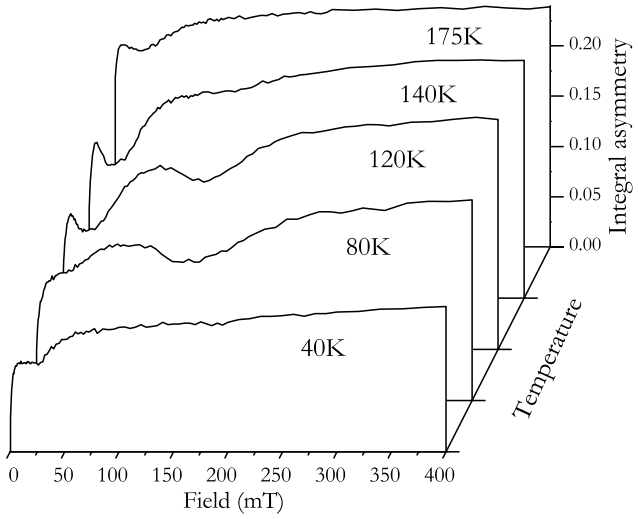

Figure 4. Evolution of the repolarization curves with temperature for Ag_2O, recorded at ISIS. Compared with the 120 K data of figure 2(b), the Mu^{I} resonance is discernible throughout this temperature range but the Mu^{II} resonance only between 80 and 140 K. A substantial fraction of the muon polarization remains missing (unrecovered in 0.4 T) around 40 K.

is not a technique which is available to conventional magnetic resonance and it is rather remarkable that anisotropic centres, formed slowly or transiently in polycrystalline material, can be characterized so successfully with time-average measurements.

4.2. Progressive delocalization of the wavefunction

Figure 4 shows a fascinating evolution of the Mu^{I} and Mu^{II} resonances in Ag_2O between selected temperatures, representing the effects of state-conversion and ionization. Our full data set up to 300 K and 400 mT is given as a contour plot of time-integral muon polarization in figure 5(a). Since the strength of $\Delta M = 1$ resonances depends on anisotropy, the effects of motional or reorientational dynamics may be folded in here. There are also indications of the involvement of a third state, Mu^{III}, whose hyperfine constant is higher, though difficult to determine from these data. This is apparent in the form of the high-field repolarization throughout much of the temperature range and more obviously from the particularly severe loss of integrated polarization in a narrow temperature range around 40 K. Whereas at both higher and lower temperatures repolarization is virtually complete in a longitudinal field of 0.4 T, at this temperature the integrated polarization is only partially recovered. In the time-domain signal this is seen to be associated with a depolarization rate of about 2 μs^{-1} over the entire field range accessible to us at ISIS, suggestive of a dynamical process with a correlation time less than $1/(\gamma_e \times 0.4\mathrm{T}) \sim 80$ ps.

Using the higher fields available at the PSI Swiss Muon Source, a broad $\Delta M = 1$ level-crossing resonance associated with this third state could be identified around 2 T. Shown in figure 5(b), the associated hyperfine parameters are $A_{iso} \sim 0.5$ GHz and $D \geqslant 0.3$ GHz. Crucially, the resonance is strongest in the vicinity of 40 K—exactly the temperature where polarization is missing in the ISIS data of figure 2(b). As an overall interpretation of these data, we are led to propose a reaction sequence,

$$Mu^{III} \rightarrow Mu^{II} \rightarrow Mu^{I}, \tag{4}$$

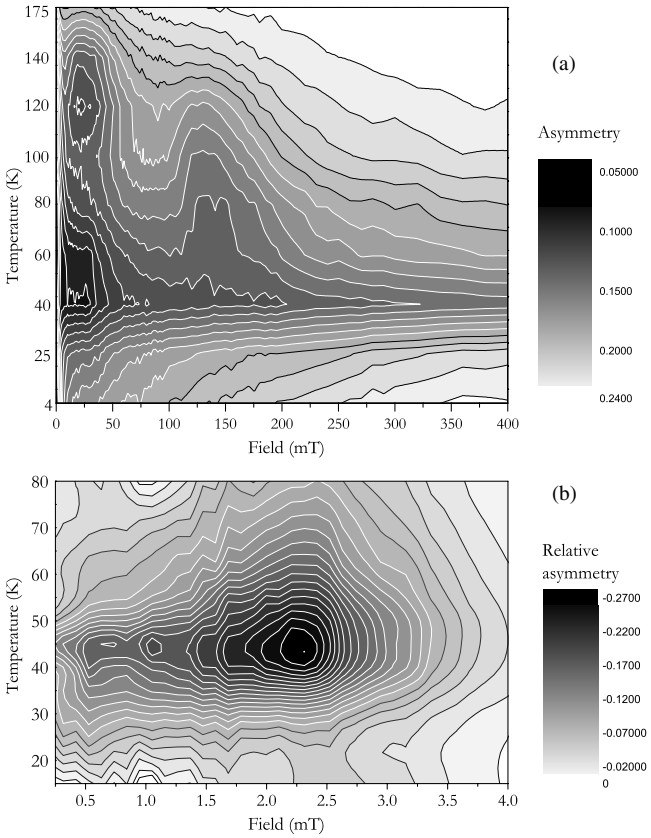

Figure 5. Contour-plots of time-average muon polarization in Ag_2O (dark grey = low, light grey = high). This is a novel representation of μSR data that succinctly represents the combined effects of all static and dynamic terms in the muonium spin Hamiltonian. The low-field resonances are apparent in the ISIS data (a), as well as the missing polarization in the vicinity of 40 K, at which temperature the high-field resonance is strongest in the PSI data (b).

with associated contact terms decreasing as

$$0.5\ \text{GHz} \rightarrow 35\ \text{MHz} \rightarrow 7\ \text{MHz}. \tag{5}$$

The rate constants are estimated (from the fitted curve in figure 2(b))[8] to be of order 2 ns^{-1} for the first step and 10 μs^{-1} for the second, at 120 K. This picture of the interconversion is not unique: the fitted curve in figure 2(b) suggests a hyperfine constant closer to 2 GHz for the parent state, more appropriate to normal or quasi-atomic muonium (compare data for Cu_2O below). Nonetheless this interplay of several muonium states appears to be a remarkable example of progressive delocalization of the unpaired electron orbital, that is, of a deep-to-shallow transition or some other solid-state reaction in operation on the sub-microsecond timescale.

[8] Procedures for the simulation and fitting of repolarization and resonance data in the presence of state transitions and spin dynamics are described elsewhere (Lord 2006, Lord *et al* 2006).

4.3. Comparison with the hydrogenic model for Ag_2O

The final state Mu^I having the lowest hyperfine constant, we consider whether it qualifies as a shallow donor in the effective mass model, in which case the Kılıç and Zunger (2002) prediction would be borne out. The electron effective mass is given as 0.7 in Ag_2O by Madelung 1996, but its dielectric constant is not tabulated in standard tables. Taking the larger activation energy of 0.25 eV in figure 2(a) as referring to the donor ionization, equation (2) implies a dielectric constant of $\varepsilon_r \approx 6$ for this material. This is not impossible: it seems more reasonable, for instance, than the value of 1.65 given by Atwater (2002), which is surely too low and may refer to solutions of Ag_2O. A donor depth of 0.25 eV is not particularly shallow, but both the loss of the Mu^I resonance in figure 4 and recovery of the Mu^+ signal in figure 2(a) imply that carrier release is complete by room temperature.

5. Cu_2O

Cuprous or copper (I) oxide, Cu_2O, was amongst the first known semiconductors; it has a direct band-gap of 2.2 eV at cryogenic temperatures and the cuprite structure is responsible for peculiar excitonic properties (Madelung 1996). Our sample was a mosaic of slices cut from a single-crystal boule, prepared by one of us (DP) at Oxford University. Paramagnetic muonium is formed when positive muons are implanted into this material, but its spectroscopy and dynamics are both very different from those in Ag_2O. Quite contrary to the data of figure 2(a), the diamagnetic fraction in Cu_2O is essentially constant at about $\frac{1}{3}$ from 4 K to well above room temperature. That is, one muon in three fails to pick up an unpaired electron, presumably thermalizing as the positive ion. The low damping of the Larmor precession signal indicates that these muons adopt crystallographic sites some distance from the copper nuclei (nuclear magnetism being relatively strong for copper but particularly weak for oxygen, in natural isotopic abundance). With values around 0.025 μs^{-1}, this damping—or, equivalently, the linewidth of the muon spin rotation spectrum—is in fact surprisingly low[9]. Evaluating the relevant dipolar sums (and with due regard for possible quadrupole interactions on the Cu nuclei) we find no candidate muon site within the undefective cuprite unit cell that can account for such a low value. Trapping at Cu vacancies is a possibility; otherwise the spectrum is motionally narrowed, implying fast muon diffusion even at cryogenic temperatures

5.1. Repolarization

The polarization that is missing in the transverse-field Larmor precession signal is entirely recovered in a longitudinal field of several hundred mT, both above room temperature and below about 70 K. (At intervening temperatures, time-average measurements exhibit some loss of polarization due to longitudinal or spin–lattice relaxation.) Figure 6(a) shows the 50 K data set: the form of the recovery is seen to be monotonic, with no sign of the dips or resonances seen for Ag_2O. This indicates that the various terms of the muonium hyperfine interaction are successively decoupled and that no level crossing resonances fall within this field range: such data are variously known as repolarization, decoupling or quenching curves. If the only term to be decoupled were a contact interaction, i.e. a purely isotropic or scalar coupling $A_{iso}\mathbf{I}\cdot\mathbf{S}$ between the muon and electron spins, the repolarization curve would have the classic form $(0.5 + (B/B_0)^2)/(1 + (B/B_0)^2)$ (see, for example, Patterson 1988). This is the dashed line in figure 6(a), fitted to the high-field data to estimate a hyperfine field of

[9] For comparison, it is just one tenth that for muons at octahedral sites in the fcc lattice of copper metal (Hartmann *et al* 1980).

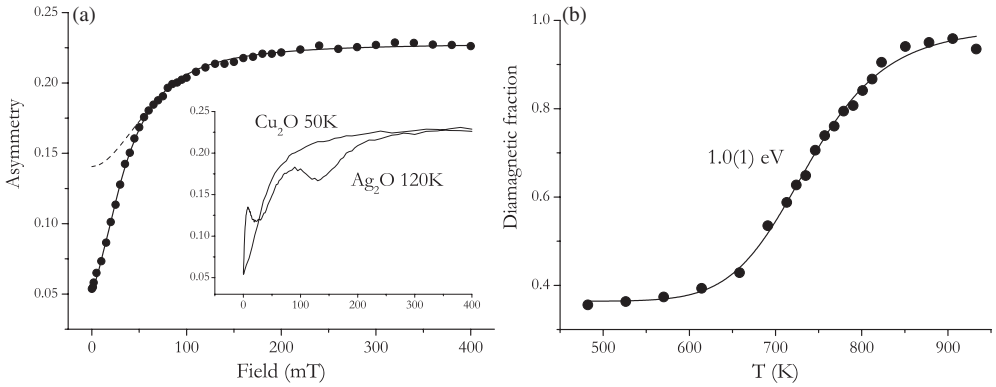

Figure 6. Recovery of muon polarization in Cu_2O in (a) longitudinal field (at 50 K) and (b) with temperature in transverse field (10 mT). The repolarization data (a) is fitted for an isotropic (quasi-atomic) muonium centre with superhyperfine interaction to an adjacent Cu nucleus (solid line). The fitted curve for an anisotropic centre is indistinguishable. The dashed curve recalls the shape for an isotropic centre with no other interactions. The inset contrasts the repolarization behaviour for Ag_2O and Cu_2O, the latter showing no level crossing resonances in this field range (these are line-plots of the data, with no fitted curves). Disappearance of neutral paramagnetic muonium is reflected by growth of the ionic diamagnetic fraction (b) and fitted for thermal ionization.

$B_0 = 2\pi A_{\rm iso}/\gamma_{\rm e} \approx 46$ mT. (B_0 may be seen to correspond to the point at which $\frac{3}{4}$ of the muonium polarization is recovered.) The corresponding contact term of $A_{\rm iso} = 1.3$ GHz is just 29% of the value for free or vacuum-state muonium (4.5 GHz), indicating a quasi-atomic muonium state in Cu_2O.

The low-field repolarization, i.e. the departure from the dashed curve in figure 6(a), can be attributed either to a degree of anisotropy or to superhyperfine interactions with Cu nuclei. The effects are rather similar and difficult to distinguish. Assuming firstly an anisotropic muonium centre with no nuclear couplings, we refine the contact term on the muon to $A_{\rm iso} = 1320 \pm 60$ MHz and fit a dipolar term of $D = -440 \pm 20$ MHz. The opposite sign of the parameters in this model is genuine: good fits cannot be obtained with the same sign for $A_{\rm iso}$ and D. This implies $|A_\perp| > |A_\parallel|$, i.e., an oblate rather than prolate hyperfine tensor.

Assuming instead an isotropic centre with nuclear superhyperfine interaction, we obtain an equally good fit to the data (indistinguishable, in fact) over the whole field range. We favour this model, since a muon–electron contact interaction only 29% of that for a 1s(Mu) configuration is rather low for such trapped-atom states, yet conspicuously similar to muonium hyperfine constants in the cuprous halides (Kiefl *et al* 1986): it suggests considerable overlap of the muonium orbital onto adjacent Cu^+ ions. Simplifying the model to interaction with a single Cu nucleus, we fit a nuclear hyperfine parameter of 210 ± 4 MHz. As a percentage of the atomic 4s(Cu) coupling of 6 GHz (Moreton and Preston 1978), it corresponds to 3.5% occupancy of the nearest Cu(4s) orbital. (Spin density in the Cu(3d) orbitals is indeterminate from the present data.) This fitting procedure gives the continuous curve in figure 6(a), and refines the muonium contact interaction to 1280 ± 20 MHz. These hyperfine parameters are entered in table 1 and discussed in the concluding section. The corresponding $\Delta M = 0$ level-crossing resonance would fall at or above 4.2 T, which is inaccessible to us but could in principle serve to check these parameters and map the local distribution of spin density. Allowance for several Cu nuclei would change the values slightly. If the centre is indeed isotropic (as it is in the cuprous halides) it must adopt a site which is symmetric with respect to several cations: the centre of the cage formed by a tetrahedron of 4 Cu atoms in the cuprite structure is the obvious candidate.

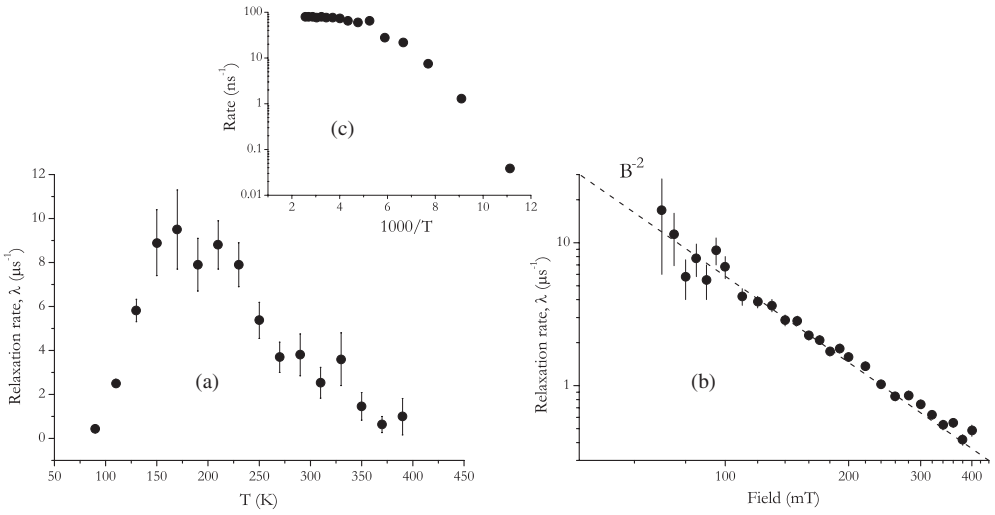

Figure 7. Variation of longitudinal relaxation rate in Cu_2O with (a) temperature (at 0.2 T) and (b) longitudinal field (at 100 K). The inferred hop-rates for muonium diffusion are given in the inset (c).

5.2. Muonium diffusion and spin–lattice relaxation

This quasi-atomic state persists from cryogenic temperatures up to beyond room temperature. It is subject to quite strong depolarization or spin relaxation, however, in a portion of this temperature range, with an onset around 100 K and a peak relaxation rate, measured in longitudinal fields, of some 10 μs^{-1} around 175 K. This relaxation peak, or T_1-minimum in NMR parlance, is shown in figure 7(a). We take it to represent spin–lattice relaxation caused by the onset of muonium diffusion, the superhyperfine interaction to Cu nuclei constituting an effective local field that acts on the unpaired electron and fluctuates as the muonium atom hops from site to site. The effect is transmitted to the muon spin via the muon–electron hyperfine interaction and so is suppressed as this interaction is decoupled in high field: figure 7(b) shows the characteristic inverse square law dependence. The muonium hop rate, analysed in this model using procedures described by Cox and Sivia (1994), is shown in the inset (c). Hop rates vary over 4 decades, up to 100 ns^{-1}, but do not show a simple Arrhenius temperature dependence; the asymptotic activation energy is about 0.1 eV at low temperature. If the static centre were anisotropic, the onset of motion could instead induce spin–lattice relaxation via reorientation of the muonium hyperfine tensor (Harshman 1986).

Some of the (lower temperature) data show an initial *increase* of relaxation rate with applied field. This is quite unusual and suggests that modulation of spin density on the muon itself, rather than on the surrounding nuclei, is the dominant relaxation mechanism: the initial variation with field should then take the form $B^2/(B^2 + B_0^2)$, this mechanism being ineffective in zero field (Cox and Sivia 1997). It would imply that the muonium visits inequivalent sites and experiences different contact interactions in the course of its diffusion. Whatever the relaxation mechanism, it seems likely that the motion is long-range at these temperatures, although it is worth recalling evidence for local tunnelling of muonium in the cuprous halides (Cox 1987, Schneider *et al* 1992).

5.3. High-temperature ionization

Figure 6(b) shows the disappearance of paramagnetic muonium between 600 and 900 K, inferred from the growth of the diamagnetic fraction towards unity[10]. The fitted activation energy is 1 ± 0.1 eV, so that artefacts of muonium diffusion and defect trapping can reasonably—though not entirely—be excluded. This value is close to half the band-gap ($E_g \approx 2.2$ eV in Cu_2O), yet there is no onset of significant spin relaxation at high temperature, whether in longitudinal or null magnetic field, that could be ascribed to interaction with intrinsic charge carriers. The disappearance of the muonium fraction appears to correspond to a clean one-way charge-state transition, therefore, defining an electrically active level close to midgap.

Whether this transition represents hole ionization or electron ionization (i.e. a deep-acceptor or a deep-donor function), however, cannot be determined from the present data. Hole ionization would imply that the high-temperature state is Mu^-, mimicking the hydride ion. Although a small increase in linewidth (transverse relaxation rate) is just discernible above 700 K, it is insufficient to claim a site adjacent to cation nuclei. Motional narrowing unfortunately precludes identification of the site and charge state at these temperatures.

6. PbO, RuO_2 and CuO

We include here a mention of some negative results, for three materials in which no neutral, paramagnetic muonium of any description could be detected, from room temperature down to about 5 K. These are PbO, RuO_2 and CuO, all of which are predicted by Kılıç and Zunger (2002) to exhibit hydrogen-induced n-type conductivity, on the basis of their pinning rule. In none of these materials, however, could we find any hyperfine splitting or broadening of the muon Larmor precession signal that might indicate the formation of shallow-donor muonium states. Neither is there any indication of normal, i.e. atomic, muonium formation, since the Larmor precession signals account for the full incoming muon polarization in each case.

For PbO, a semiconductor with an indirect gap of 1.9 eV in its red tetragonal form, this is unexpected. Assuming the implanted muons thermalize as positive ions, electrons should be weakly bound as hydrogenic donors at cryogenic temperatures even if a deep or localized atomic centre is not formed. We note a similarly puzzling absence of any paramagnetic muonium centre in the wider-gap PbO_2. For RuO_2, on the other hand, the negative result comes as no surprise: this material is essentially metallic, so that screening of the charge defect by mobile conduction electrons is likely to preclude formation of a paramagnetic centre with long-lived spin states. Hydrogen doping would not appear to be a relevant issue in this material—nor in IrO_2, which is undoubtedly metallic, yet nevertheless also figures amongst Kılıç and Zunger (2002) predictions.

We include here a brief comment on cupric or copper (II) oxide, CuO. This is a material of uncertain band-gap[11] but which is also magnetic. Contrary to the closed-shell configuration of Cu^+, the $3d^9$ configuration of Cu^{2+} carries a moment of about 1 Bohr magneton, giving rise to long-range magnetic ordering in CuO below about 230 K. Muonium would be difficult to recognize in an ordered magnetic phase, being subject to strong depolarization by the atomic moments, especially when these exhibit magnetic fluctuations[12]. Of course, in magnetic oxides

[10] A sintered polycrystalline sample was used for these furnace measurements. The cuprite structure is said to be metastable above room temperature, but we have no evidence of transformation of the sample beyond reduction of a thin surface layer to metallic copper. This layer was too thin to stop muons, so that the curve of figure 6(b) is reversible.

[11] The band-gap is given as 1.6 eV by Schmickler and Schultze (1986) although, according to Madelung (1996), no transparency gap is found in the visible or near infra-red.

[12] Exceptionally, Luke *et al* (1986), Kiefl *et al* (1987) were able to deduce the presence of atomic muonium in MnF_2.

as in other magnetic materials, the muon spin (usually presumed associated with the Mu^+ ion) offers a unique probe of internal fields and their fluctuation rates. CuO is no exception and the papers by Niedermeyer *et al* (1988), Duginov *et al* (1994), Nishiyama *et al* (2001) all show how μSR data has contributed to elucidating the antiferromagnetic order.

A crystal of CuO being available to us (also prepared by DP at Oxford University), we undertook a search for atomic muonium in the paramagnetic phase but found no evidence for it. The muon Larmor precession signal has its maximum possible amplitude from room temperature down to the magnetic transition. Neutral muonium, if present, must be subject to such rapid spin exchange as to be indistinguishable from the locally diamagnetic Mu^+ or OMu^- ions. We certainly do not expect to be able to test for a shallow-donor muonium states under such conditions and have otherwise excluded magnetic oxides from our survey.

7. Concluding remarks

Our hyperfine parameters for muonium in CdO, Ag_2O and Cu_2O are compared in table 1 with those for different categories of muonium centre in other semiconductors. With the reservations expressed above, the weakly bound paramagnetic state found in CdO and the centre denoted Mu^I in Ag_2O appear to qualify as effective-mass donors. For CdO, there is no sign of any coexisting acceptor state, so our data support the predictions of Kılıç and Zunger (2002) for this material: hydrogen could indeed be an adventitious dopant and cause of n-type conductivity. For Ag_2O, there is undoubtedly metastability, but the resultant electrical activity is somewhat unclear. The Mu^{II} centre is probably a deep donor although, since ionization is complete by room temperature the distinction between shallow and deep donors is unimportant here for most practical purposes: the question is whether the electrons released by analogous H^I and H^{II} centres remain available for conduction or are trapped by H^{III}. We find no paramagnetic muonium centres, deep or shallow in PbO, nor in RuO_2. For PbO, this may be a question of sample purity or quality but for RuO_2 we contest the prediction, this material being essentially metallic.

In CdO, the shallow-donor state of muonium appears to be somewhat more compact and tightly bound than is expected for a simple hydrogenic centre, apparently governed by the optical rather than the static dielectric constant. The result is somewhat surprising, since the usual effective mass approximation works well, for instance, for substitutional donors in CdTe. The difference between the static and optical dielectric constants is unusually great for CdO, however, and it may be that the disparity between anion and cation masses makes ionic screening less effective in the oxide. Hydrogen and muonium are not subject to core effects in the usual sense; nevertheless variation of the Bloch-wave amplitudes may give significant deviations from the hydrogenic theory for charge defects at interstitial sites. Alternatively, it may simply be that hydrogen and muonium are particularly close to the shallow-to-deep instability in CdO, only just qualifying for the effective-mass model.

For the transient state Mu^{II} in Ag_2O, a dipolar parameter of $D = 10$ MHz implies that the unpaired electron spin is localized at an average distance of 0.3 nm (3 Å) from the central muon. Together with the low contact interaction, this points to a more extended orbital than that for the $^{\cdot}(AgH)^+$ radical cation proposed by Eachus and Symons (1969, 1970). The alternative species mooted by these authors, $^{\cdot}(Ag–H–Ag)^{2+}$, provides a somewhat closer match with our muonium hyperfine parameters: it would account for the low contact interaction, if the muon occupies a bridging site and lies at a node of the electronic orbital in the manner of bond-centred muonium and hydrogen in silicon.

As an intermediary in the reduction of Ag^+ cations by atomic hydrogen, represented by reaction-sequence (6), the radical cation lives less than 10 ps in aqueous solution, according to

Tausch-Treml *et al* (1978). Making the analogy with our sequence $Mu^{III} \rightarrow Mu^{II} \rightarrow Mu^{I}$, this reaction still proceeds, though more slowly, in the solid state at cryogenic temperatures[13].

$$Ag^{+} + H^{0} \rightarrow {}^{\cdot}AgH^{+} \rightarrow Ag^{0} + H^{+}. \tag{6}$$

In fact, it seems clear from our own data that (in solid Ag_2O) the unpaired electron delocalizes further. The complex $[Ag^0\,H^+]$ would be classed as a deep polaron and is an alternative assignment for our transient intermediary Mu^{II}.

We have no evidence for muonium forming effective-mass donors in Cu_2O. This material has $\varepsilon_r \approx 7$ and an electron effective mass of $m^*/m_e = 0.91$ (Madelung 1996), leading to an expected binding energy of $R_y \times m_n/\varepsilon_r^2 = 13.6 \times 0.9/7^2 = 0.25$ eV. The volume dilation in the hydrogenic model is likewise $(a^*/a_0)^3 = (\varepsilon_r/m_n)^3 = 440$, giving a simplistic estimate of muonium hyperfine constant as $A_0 \cdot (a^*/a_0)^{-3} \approx 10$ MHz.[14] There are no discernible features in any of our data which could correspond to such a centre. Instead, a quasi-atomic state is found that is stable to well above room temperature, eventually disappearing with an effective ionization energy of 1 eV. With a hyperfine constant just 29% of the free-atom value, this muonium state in Cu_2O bears a strong resemblance to the isotropic muonium centres known in the cuprous halides, CuCl, CuBr and CuI, for which the values range from 27% to 37% (Kiefl *et al* 1986, Schneider *et al* 1990). These are even lower than the 50% for cage-centred muonium, Mu_T, in Si and are in fact amongst the lowest hyperfine constants known for otherwise atomic-like muonium centres: see, for instance, the compilations by Schneider *et al* (1986) or Cox (1987, 2003). The insensitivity of the coupling to the identity of the anion suggests involvement of the cation d-orbitals, which are unusually accessible for Cu^+. A version of the ${}^{\cdot}(CuMu)^+$ radical-cation model, proposed for the cuprous halides by Cox and Symons (1986), appears equally appropriate to Cu_2O, therefore. Location of the muonium atom at the tetrahedral interstitial site (in the fcc sublattice of cuprite), with its wavefunction spreading symmetrically onto four Cu atoms, would ensure the isotropy. This site would also be a favourable location for the negative ion that may well be the product of the high-temperature charge-state transition. The present data are unable to distinguish, however, between an acceptor and donor function for the approximately mid-gap level.

In conclusion, the three oxides CdO, Ag_2O and Cu_2O illustrate the wide variety paramagnetic centres that muonium—and by inference hydrogen—can adopt in semiconductors. The hyperfine spectroscopy of muonium is surprisingly rich in these few materials. The shallow state in CdO supports first-principles predictions but raises questions about the validity of the effective-mass or hydrogenic model for the interstitial shallow-donor state. The metastability of the muonium states in Ag_2O and the unusually low spin-density in the deep quasi-atomic state in Cu_2O all require further elucidation, e.g. by first-principles computation. Our survey extends to wide-gap and high-permittivity oxides in the accompanying paper (II), where a similar variety of electronic structures is found and the systematics of the shallow-to-deep instability begin to emerge.

Acknowledgments

Discussions with A Sokol, E A Davis and E Roduner are gratefully acknowledged. The data were recorded in successive allocations of muon beamtime during 2003 and 2004 at the CCLRC

[13] This seems more plausible than the opposite hypothesis of oxidation of Ag(I) to Ag(II), implied by Eachus and Symons (1970), who write the ${}^{\cdot}(AgH)^+$ configuration as $Ag^{2+}H^-$. Their suggestion raises the question as to whether hydrogen is in fact playing the rôle of acceptor rather than donor here, but is in our view unlikely.

[14] This scaling with the volume of the hydrogenic orbital fails if positive spin density on the muon is precluded by the high energy of the OH antibonding orbital; if there is no occupation of this antibonding orbital, the contact term must instead be negative, representing spin-polarization of the doubly occupied bonding orbital.

ISIS Facility (EMU, MuSR and DEVA instruments) and at the Swiss Muon Source PSI (GPD and ALC instruments). The Coimbra Group acknowledges support by FCT/FEDER European Funds (grant POCTI/35334/FIS/2000-Portugal).

References

Alberto H V, Vilão R C, Piroto Duarte J, Gil J M, Ayres de Campos N, Lichti R L, Davis E A, Cottrell S P and Cox S F J 2001 *Hyperfine Interact.* **136/137** 471
Atwater J E 2002 *Appl. Phys.* A **75** 555
Bech Nielsen B, Johannesen P, Stalinga P, Bonde Nielsen K and Byberg R J R 1997 *Phys. Rev. Lett.* **79** 1507
Brewer J H, Crowe K M, Gygax F N and Schneck A 1975 *Muon Physics* vol 3, ed V W Hughes and C S Wu (New York: Academic) p 3
Chow K H, Hitti B, Kiefl R F, Lichti R L and Estle T L 2001 *Phys. Rev. Lett.* **87** 216403
Cox S F J 1987 *J. Phys. C: Solid State Phys.* **20** 3187
Cox S F J 2003 *J. Phys.: Condens. Matter* **15** R1727
Cox S F J, Davis E A, Cottrell S P, King P J C, Lord J S, Gil J M, Alberto H V, Vilão R C, Piroto Duarte J, Ayres de Campos N, Weidinger A, Lichti R L and Irvine S J C 2001a *Phys. Rev. Lett.* **86** 2601
Cox S F J, Davis E A, King P J C, Gil J M, Alberto H V, Vilão R C, Piroto Duarte J, Ayres de Campos N and Lichti R L 2001b *J. Phys.: Condens. Matter* **13** 9001
Cox S F J, Cottrell S P, Lord J S, Vilão R C, Alberto H V, Piroto Duarte J, Gil J M, Ayres de Camps N, Davis E A, Charlton M, Van der Werf D P, Keeble D J, Lichti R L and Weidinger A 2005a *Proc. ICPS27 (Flagstaff, July 2004)*; *AIP Conf. Proc.* **772** 193
Cox S F J, Gavartin J L, Lord J S, Cottrell S P, Gil J M, Alberto H V, Piroto Duarte J, Vilão R C, Ayres de Campos N, Keeble D J, Davis E A, Charlton M and Van der Werf D P 2006 *J. Phys.: Condens. Matter* **18** (Accompanying paper on widegap oxide dielectrics, referred to in the text as Paper II)
Cox S F J, Lord J S, Cottrell S P, Alberto H V, Piroto Duarte J, Vilão R C, Keren A and Prabhakaran D 2005b *Proc. HFI2004 (Bonn, Aug. 2004)*; *Hyperfine Interact.* at press (doi:10.1007/510751-005-9058)
Cox S F J and Sivia D S 1994 *Hyperfine Interact.* **87** 923
Cox S F J and Sivia D S 1997 *J. Appl. Magn. Reson.* **12** 213
Cox S F J and Symons M C R 1986 *Chem. Phys. Lett.* **126** 516
Davis E A, Cox S F J, Lichti R L and Van de Walle C G 2003 *Appl. Phys. Lett.* **82** 592
Dickson W R 1999 *PhD Thesis* Southampton University
Duginov V N *et al* 1994 *Hyperfine Interact.* **85** 317
Eachus R S and Symons M C R 1969 *Chem. Commun.* 285
Eachus R S and Symons M C R 1970 *J. Chem. Soc.* A 1336
Gil J M, Alberto H V, Vilão R C, Piroto Duarte J, Ayres de Campos N, Weidinger A, Krauser J, Davis E A, Cottrell S P and Cox S F J 2001a *Phys. Rev.* B **64** 075205
Gil J M, Alberto H V, Vilão R C, Piroto Duarte J, Ayres de Campos N, Weidinger A, Davis E A and Cox S F J 2001b *J. Phys.: Condens. Matter* **13** L613
Glover C, Newton M E, Martineau P M, Quinn S and Twitchen D J 2004 *Phys. Rev. Lett.* **92** 135502
Harshman D R 1986 *Hyperfine Interact.* **32** 847
Hartmann O *et al* 1980 *Phys. Rev. Lett.* **44** 337
Hofmann D M, Hofstaetter A, Leiter F, Zhou H, Henecker F, Meyer B K, Orlinskii S B, Schmidt J and Baranov P G 2002 *Phys. Rev. Lett.* **88** 045504
Hogarth C A 1951 *Proc. Phys. Soc. London* B **64** 691
Jarzebski Z M 1969 *Bulletin de l'Académie Polonaise des Sciences* (*Série des Science Chimiques* vol 17) p 221
Jarzebski Z M 1973 *Oxide Semiconductors* (*International Series of Monographs on the Solid State* vol 4) (Oxford: Pergamon) (ISBN 0-08-016968-6)
Kiefl R F *et al* 1986 *Phys. Rev.* B **34** 1474
Kiefl R F *et al* 1987 *Phys. Rev.* B **35** 2079
Kiefl R F, Celio M, Estle T L, Kreitzman S R, Luke G M, Riseman T M and Ansaldo E J 1988 *Phys. Rev. Lett.* **60** 224
Kılıç Ç and Zunger A 2002 *Appl. Phys. Lett.* **81** 73
Koffyberg F P 1976 *Phys. Rev.* B **13** 4470
Kreitzman S R and Roduner E 1995 *Chem. Phys.* **192** 189
Lichti R L, Chow K H, Davis E A, Hitti B H, Celebi Y G and Cox S F J 2003 *Physica* B **326** 167
Lord J S 2006 Computer simulation of muon spin evolution *Proc. μSR 2005 (Oxford, Aug. 2005)*; *Physica* B at press

Lord J S, Cottrell S P, King P J C, Alberto H V, Ayres de Campos N, Gil J M, Piroto Duarte J, Vilão R C, Lichti R L, Sjue S K J, Bailey B A, Davis E A and Cox S F J 2001 *Physica* B **308–310** 920–3
Lord J S, Scheuermann R, Cox S F J and Stoykov A 2006 Muonium states in Ag_2O studied by level crossing and RF resonance *Proc. μSR 2005 (Oxford, Aug. 2005)*; *Physica* B at press
Luke G M *et al* 1986 *Hyperfine Interact.* **31** 29
Madelung O (ed) 1996 *Semiconductors—Basic Data* (Berlin: Springer)
Moreton J R and Preston K F 1978 *J. Magn. Reson.* **30** 577
Niedermeyer Ch *et al* 1988 *Phys. Rev.* B **38** 2836
Nishiyama K *et al* 2001 *Hyperfine Interact.* **136/137** 289
Patterson B D 1988 *Rev. Mod. Phys.* **60** 69
Ridley B K 1982 *Quantum Processes in Semiconductors* (Oxford: Clarendon)
Roduner E 1999 *Muon Science* ed S L Lee *et al* (Bristol: Scottish Universities Summer School in Physics and Institute of Physics Publishing) p 173
Schefzik M *et al* 2000 *Physica* B **289/290** 511
Schmickler W and Schultze J W 1986 *Modern Aspects of Electrochemistry* vol 17 (New York: Plenum) pp 357–410
Schneider J W *et al* 1986 *Hyperfine Interact.* **32** 607
Schneider J W *et al* 1990 *Phys. Rev.* B **41** 7254
Schneider J W *et al* 1992 *Phys. Rev. Lett.* **68** 3196
Shimomura K, Nishiyama K and Kadono R 2002 *Phys. Rev. Lett.* **89** 255505
Stoneham A M and Dhote J 1997 *Crystal Data* (see www.oxmat.co.uk/Crysdata)
Storchak V G, Eshchenko D G and Brewer J H 2004 *J. Phys.: Condens. Matter* **16** S4767
Tausch-Treml R, Henglein A and Lilie J 1978 *Ber. Bunsenges. Phys. Chem.* **82** 1335
Van de Walle C G 2000 *Phys. Rev. Lett.* **85** 1012